

Studies on Tin and Iron doped TiO₂ thin films prepared by Sol-gel dip coating technique

R.Rajeswari *, D.Venugopal

Research Department of Physics,
Gobi Arts & Science College, Gobichettipalayam.

Abstract

Tin and Iron doped TiO₂ thin films were prepared on glass substrate by sol-gel process and dip coating technique. The coating solution was prepared by using Titanium-Tetra Isopropoxide (TTIP) precursor. Very stable sols of this oxide were synthesized in the presence of HNO₃ and using N-N Dimethyl Formamide (DMF) as a solvent. The prepared thin films are uniform and having good adhesion to the glass substrate. The thickness of the deposited films varied from 100 to 200 nm depending on the coatings number. The morphological characteristics and structures of Tin and Iron doped TiO₂ thin films were examined by X-Ray Diffraction (XRD), Scanning Electron Microscopy (SEM) and Energy Dispersive Spectroscopy (EDS). The optical transmission spectra were calculated in the wavelength region 300nm-1200nm. The optical band gap of the Tin and Iron doped TiO₂ thin films was found to be 3.488eV and 3.375eV respectively. Dielectric properties of both the films were studied as a function of frequency at different temperatures (50°C & 200°C). The material displays high dielectric constant and dielectric loss at low frequencies and it becomes low when the frequency reaches to a high value.

Keywords: Sol-gel method, Sn/Fe doped TiO₂, Dip coating, Thin Films.

1.Introduction

Enormous efforts have been devoted to the research of Titanium dioxide (TiO₂) [1-3]. TiO₂ is widely used in various scientific and technological fields due to properties such as non-toxicity, chemical stability, low cost and optical properties [4,5]. All these TiO₂ properties can be applied in different areas of research such as fabrication of dye sensitized solar cells(DSSCs) [6,7], production of gas sensors [8,9], photocatalysis [10,11], water purification [12,13], self cleaning and self sterilizing materials[14,15].TiO₂ is an n-type semiconductor which can be found in any of its three polymorphs: anatase(tetragonal), brookite(ortho-rhombic) and rutile (tetragonal) . TiO₂ thin films can be transformed from amorphous phase into crystalline anatase and from anatase into rutile by temperature treatment [16]. TiO₂ thin films have been synthesized using various techniques such as evaporation [17], sputtering [18,19], spray pyrolysis [20-22], sol-gel [23,24], spin coating [25,26], dip coating [27,28] and other methods. Sol-gel dip coating technique is widely used in the fabrication of TiO₂ thin films owing to its simplicity of operation, performed at low temperature, efficiency and practicality. Dip coating technique can be described as a process where the substrate to be coated is immersed in a liquid and then with drawn with a well defined withdrawal speed under controlled temperature and atmospheric conditions. The coating thickness is mainly defined by the withdrawal speed by the solid content and the viscosity of liquid. This process does not require a costly vacuum system since the coating process can be conducted under air [29]. Titania thin films prepared in this way can be of high purity, cost effective and simple procedure.

This work reports on the studies of Sn doped TiO₂ and Fe doped TiO₂ thin films produced by sol-gel route. Moreover, due to advantage of the sol, annealing caused to formation of only one phase (anatase) for both Sn and Fe doped TiO₂ thin films. Sol-gel technique can give a better control of particle size and homogeneity in the particle distribution [30]. The properties of the sol-gel TiO₂ thin films are highly dependent on the structure (amorphous or crystallized), the thickness and the density of the deposited layers. These features are then mainly influenced by the sol composition, the sol viscosity, the withdrawal speed, the substrate nature and the sintering mode [31,32]. The main difficulty encountered with TiO₂ is the high recombination rate of the photo excited electron hole pairs in the irradiated particles [33]. This problem can be resolved by changing the structure of photocatalyst by doping with Tin and Iron or other metal. However, the doped TiO₂ thin films have shown potential for uses in number of electronic device applications. Additionally, good dispersibility of TiO₂ is very advantageous in enhancing their UV screening efficiency [34]. The high dielectric constant of TiO₂ allows its considerations as an alternative to silicon dioxide for ultra thin gate oxide dielectrics used in memory and logic devices. The dielectric properties of TiO₂ have been of great interest for applications in the telecommunications industry due to its unusual high dielectric constant and low dielectric loss. Doping TiO₂ with Sn and Fe or other metal ions shifts the threshold for photonic excitation towards the visible range [35]. Fe ions doped into TiO₂ have caused changes in phase composition and some properties of the catalyst such as phase composition, particle size and surface area [36].

2. Experimental

2.1. Materials

Titanium tetra Isopropoxide (TTIP, 97%, Sigma-Aldrich) was used as a precursor and Dimethyl formamide (DMF, 99%, LOBAL) served as a solvent. Nitric acid (HNO_3 , 69%, Merck) was used as a catalyst. Tin (II) chloride ($\text{SnCl}_2 \cdot 2\text{H}_2\text{O}$, 98%, Merck) and Ferric Nitrate ($\text{Fe}(\text{NO}_3)_3 \cdot 9\text{H}_2\text{O}$, 98%, LOBAL) was used as a doping agent.

2.2. Preparation of Sn doped TiO_2 sol

20ml of N-N Dimethyl formamide (DMF) was added with 1ml of Titanium – Tetra- Isopropoxide (TTIP). After stirring for 5 minutes at ambient temperature, Tin chloride was quickly added into the solution at desired molar ratios. Two drops of HNO_3 was added five times for every 10 minutes to the above mixture. This mixture was stirred at room temperature, till we obtained a Transparent yellow solution.

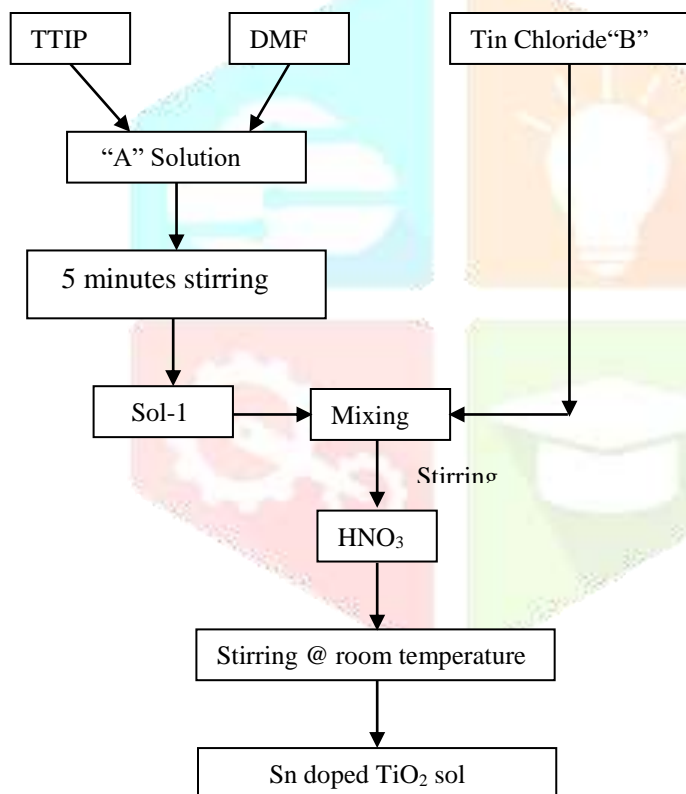


Fig (1) Flow chart for the preparation Sn doped TiO_2 sol

2.3. Preparation of Fe doped TiO_2 sol

20ml of N-N Dimethyl formamide (DMF) was added with 1ml of Titanium – Tetra- Isopropoxide (TTIP). After stirring for 5 minutes at ambient temperature, Ferric nitrate was quickly added into the solution at desired molar ratios. Two drops of HNO_3 was added five times for every 10 minutes to the above mixture. This mixture was stirred at room temperature, till we obtained a Transparent brown solution.

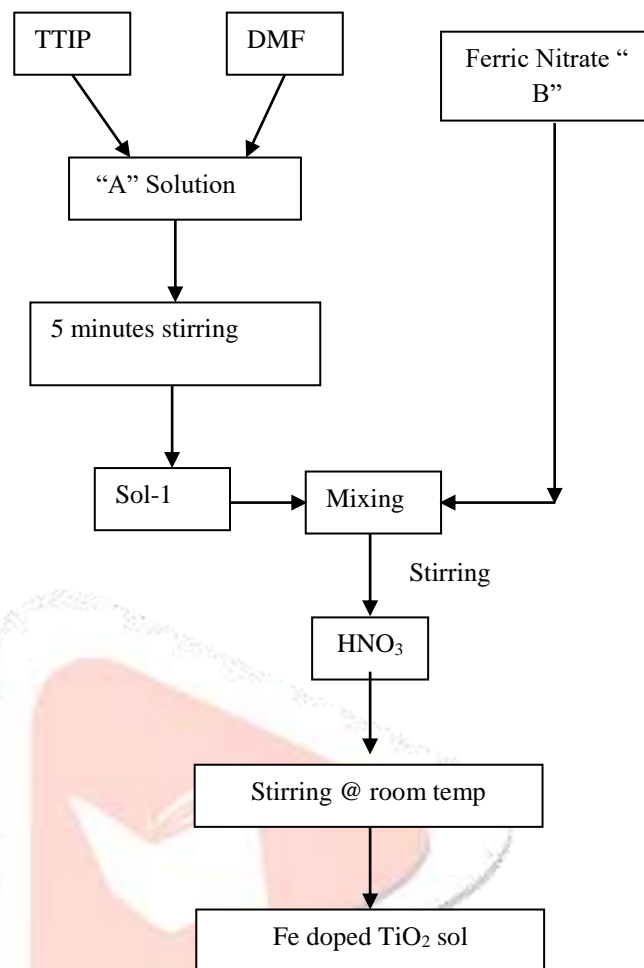


Fig (2) Flow chart for the preparation of Fe doped TiO_2 sol

2.4. Preparation of samples

Doped TiO_2 thin films were obtained by the dip coating technique. In the present work, microscopic glass slides have been used as substrates. At first, substrates were cleaned in an ultrasonic cleaner with de-ionized water and then with acetone. Subsequently the well cleaned glass substrates were immersed in the sols and then dried at 150°C

and 400°C for 1h. The deposition condition maintained to prepare Sn and Fe doped TiO_2 samples:

Substrate	: glass.
Dipping Speed	: 160.00 mm/min
Lifting Speed	: 160.00 mm/min
Length	: 18.0 mm
Wet Time	: 10 Minutes
Dry Time	: 5 minutes
Cycles	: 10 cycles
Pre- annealing time	: 1 hour

Pre – annealing temperature : 150⁰ C
 Post annealing Time : 1 hour
 Post annealing temperature : 400⁰ C

The adhesion of the films to the substrates seems to be good

2.5. Characterization of TiO₂ Films

The crystalline phase of doped TiO₂ thin films were analysed using X-ray diffractometer (XRD, D8 Advance, Bruker). Film morphology was characterized by Scanning Electron Microscopy (SEM, Tescan Model). The films elemental analysis was performed using Energy Dispersive Spectroscopy (EDS). The optical transmission spectra in the wavelength region 300nm-1200nm was recorded for doped TiO₂ thin films using perkin elmer make lambda 35 UV-Vis spectrometer. The electrical behavior of the TiO₂ films was studied over a range of frequency (1HZ-1MHZ) and temperature (50⁰ C & 200⁰ C) using an impedance analyser PSM 1735 LCR Meter.

3. Results and discussion

3.1. Structural analysis

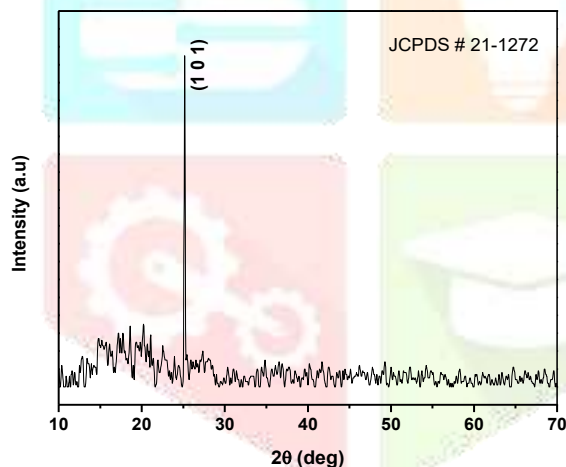


Fig (3) XRD pattern of Sn doped TiO₂ thin films

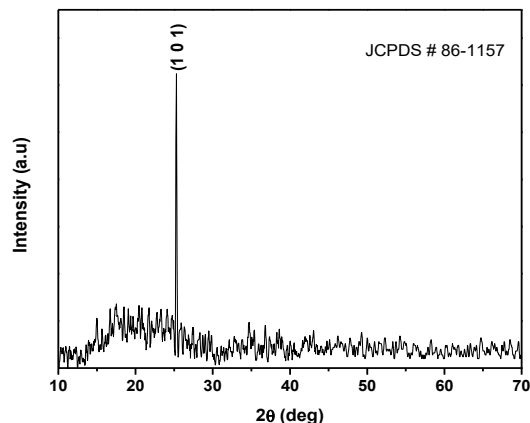


Fig (4) XRD pattern of Fe doped TiO₂ thin films

Fig (3) and (4) show the XRD pattern of Sn and Fe doped TiO₂ thin films. XRD pattern is revealed the formation of crystalline TiO₂ with tetragonal structure. The observed diffraction peaks at [1 0 1] shows anatase phase of Sn and Fe doped TiO₂ thin films, which are in good agreement with standard JCPDS card (No.21-1272) and JCPDS card (No.86-1157) respectively[37]. Sn doped TiO₂ thin films diffraction peak are slightly shifted upward when compared with the Fe doped TiO₂ thin films. The mean crystallite size of Sn and Fe doped TiO₂ thin films were calculated using Debye–Scherrer's formula given by ,

$$D = (k\lambda)/(\beta\cos\theta)$$

where, the constant 'k' is the shape factor 0.94, 'λ' is the wavelength of X-rays, 'θ' is the Bragg's angle and 'β' is the full width at half maximum of diffraction peaks measured in radians. The mean grain size (D) of Sn and Fe doped TiO₂ thin films were calculated and it comes around 59 nm and 50 nm respectively. Comparing both, the Sn doped TiO₂ is having high crystalline nature because of crystalline size have been increased.

Structural Parameters	Calculated Value	
	Sn doped TiO ₂ 2θ=25.166	Fe Doped TiO ₂ 2θ=25.288
Interplanar distance (d)	0.353×10 ⁻⁹ m	0.353×10 ⁻⁹ m
Lattice Plane [hkl]	[1 0 1]	[1 0 1]
Grain Size (D)	59 nm	50 nm
Dislocation Density (δ)	0.283×10 ¹⁵ lines/m ²	0.405×10 ¹⁵ lines/m ²
Micro Strain (ε)	5.8336×10 ⁻⁴ lines ⁻² / m ⁴	6.9818×10 ⁻⁴ lines ⁻² / m ⁴
Lattice Constants (a&c)	a=3.785 & c=9.513	a=3.785 & c=9.513

Table (1) Structural Parameters of the Sn and Fe doped TiO₂ films

3.2. Surface Analysis

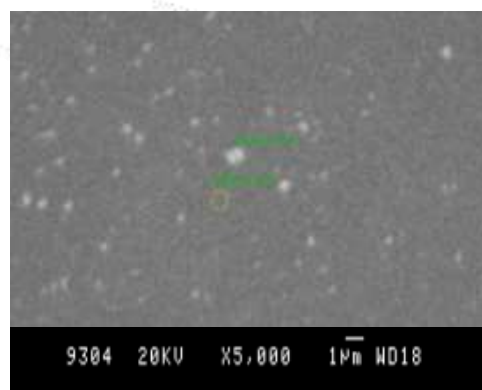


Fig (5) SEM image of Sn doped TiO₂ thin films

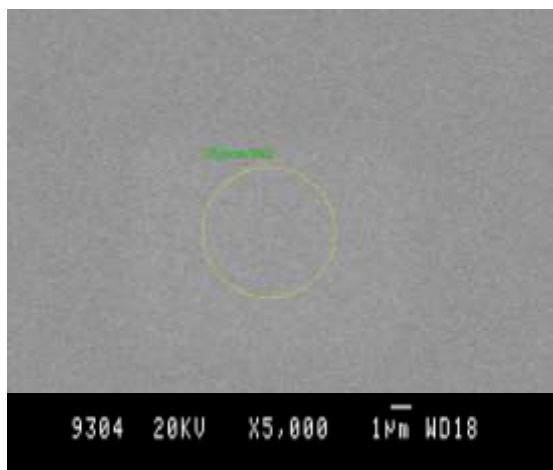


Fig (6) SEM image of Fe doped TiO₂ thin films

The SEM images presented above show that doping has improved the quality of the thin films. Doping Sn and Fe must have increased the adhesion capability of the films. The surface of both the film shows a smooth morphology. However it is evident that doping Sn into TiO₂ matrix has increased the particle size. This result is in correlation with those obtained from XRD. Fe doped TiO₂ thin films doesn't show any particles as such but Sn doped TiO₂ thin films show uniform distribution of particles covering the entire film.

3.3. Compositional analysis

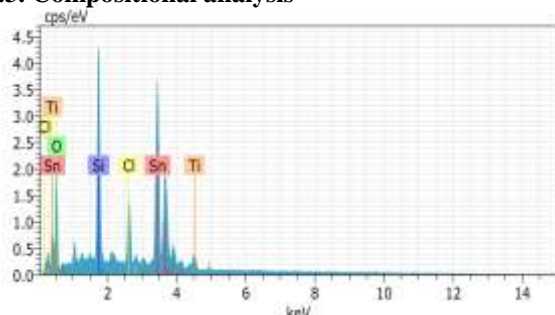


Fig (7) EDAX spectrum of Sn doped TiO₂ thin films

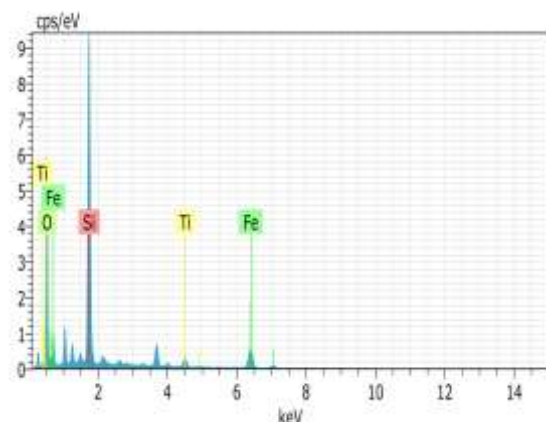


Fig (8) EDAX spectrum of Fe doped TiO₂ thin films

EDAX measurement is employed in the present study to identify the presence of titanium, Sn and Fe ions. The EDAX patterns for Sn and Fe doped TiO₂ thin films are shown in Fig (7) and Fig (8) respectively. From the area underneath the peaks, the composition of the elements present in the system can be determined. EDAX spectra of Sn doped TiO₂ thin film contains Ti, Sn elements and also some impurities were present in the sample. Similarly EDAX spectra of Fe doped TiO₂ thin film contains Ti, Fe elements and also some impurities were present in the sample due to the atmosphere.

3.4. Optical Analysis

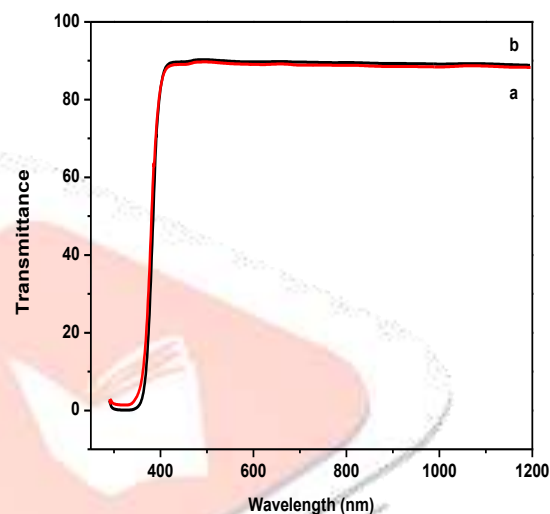


Fig (9) Transmittance spectra of (a) Sn (b) Fe doped TiO₂ thin films

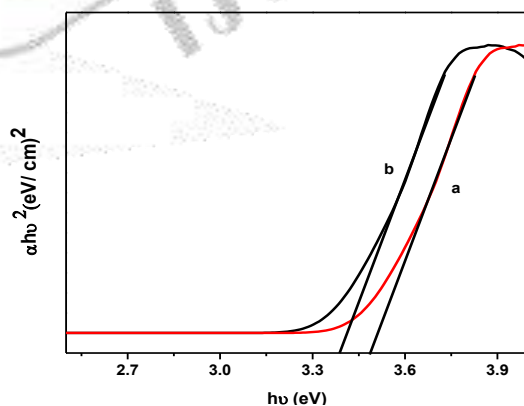


Fig (10) Tauc plot of (a) Sn (b) Fe doped TiO₂ thin films

The optical transmission spectra in the wavelength region 300nm-1200nm have been recorded for Sn and Fe doped TiO₂ thin films. Fig (9) shows the transmittance spectra of Sn and Fe doped TiO₂ thin films was recorded using perkin elmer make lambda 35 UV-Vis spectrometer and the observed spectrum corresponding to the Sn, Fe doped TiO₂ thin films.

All the films exhibited high transmittances in the range 80–90% above the absorption edge. Relatively high transmittance is a good indication of lower surface roughness and good homogeneity. However, the broad cut off towards shorter wavelength (300 nm–1200nm). The optical band gap (E_g) has been calculated using the graph plotted between $(\alpha h\nu)^2$ (eV/cm^2) Vs $h\nu$ (eV) shown in Fig (8). The optical band gap of the Sn and Fe doped TiO_2 thin films are found it around 3.488 eV and 3.375 eV respectively [38-41].

3.5. Dielectric properties

Dielectric constant is one of the basic electrical properties of solids which give details about the atoms, ions and their polarization mechanism. This technique helps us to separate the real and imaginary parts of the electrical parameters and therefore provides information about the material properties.

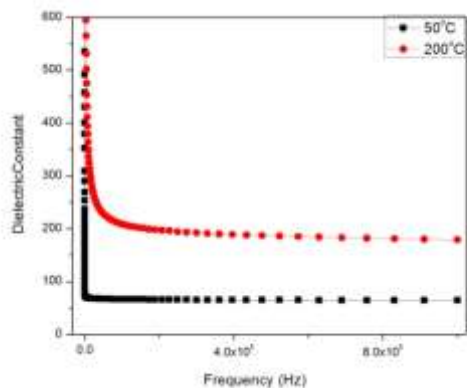


Fig (11) Variation of dielectric constant with frequency for Sn doped TiO_2 thin films

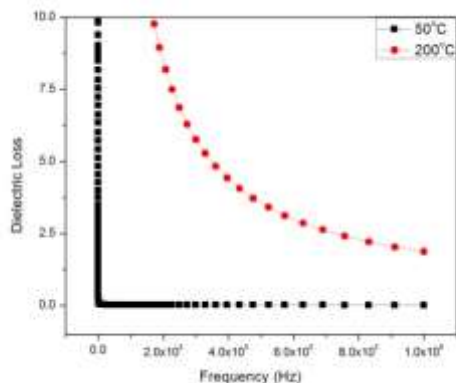


Fig (12) Variation of dielectric loss with frequency for Sn doped TiO_2 thin films

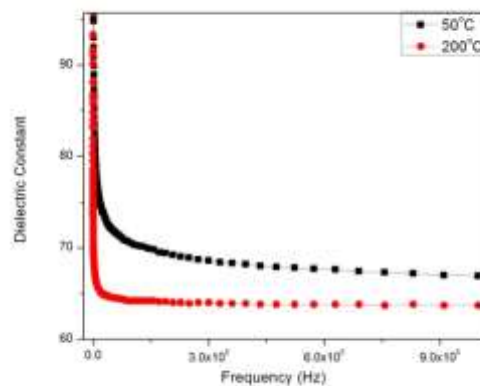


Fig (13) Variation of dielectric constant with frequency for Fe doped TiO_2 thin films

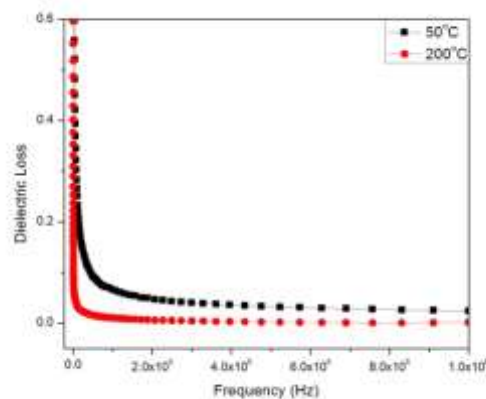


Fig (14) Variation of dielectric loss with frequency for Fe doped TiO_2 thin films

The variation of relative dielectric constant and dielectric loss measured at two different temperatures (50°C and 200°C) as a function of frequency (1Hz-1MHz) are shown in the Fig (11) & Fig (12) for Sn doped TiO_2 thin films and Fig (13) & Fig (14) for Fe doped TiO_2 thin films. From above figures, it is observed that the material displays high dielectric constant at low frequencies and it becomes low when the frequency reaches to a high value. The larger value of dielectric constant at lower frequencies is due to the presence of space charge orientation, ionic and electronic polarizations in the crystal. The very low value of dielectric constant at higher frequencies is important for the fabrication of materials towards ferroelectric, photonic and electro-optic devices. The dielectric loss is also studied as a function of frequency at two different temperatures and is shown in the above two graphs. These curves suggest that the dielectric loss is strongly dependent on the frequency of the applied field, similar to that of dielectric constant [42,43].

4. Conclusion

Thin films of Sn and Fe doped TiO_2 were deposited onto well-cleaned glass substrates by using sol-gel dip coating technique. The structure of the deposited films have been analysed by X-ray diffraction technique. The XRD pattern of

Sn and Fe doped TiO₂ thin films revealed the formation of crystalline TiO₂ with tetragonal structure. The observed diffraction peaks at [101] shows anatase phase for both Sn and Fe doped TiO₂ films. The surface morphology of the doped TiO₂ thin films were analysed by SEM. The surface of the film shows a smooth morphology, however it is evident that doping Sn into TiO₂ matrix has increased the particle size. EDS spectra of Sn and Fe doped TiO₂ thin film contains Ti, Sn and Ti, Fe respectively.

The optical related parameters were calculated from the transmittance spectra. The optical band gap of the Sn and Fe doped TiO₂ thin films are found to be 3.488 eV and 3.375 eV respectively. Dielectric properties of Sn and Fe doped TiO₂ thin films were studied as a function of frequency at different temperatures (50°C & 200°C). The material displays high dielectric constant and dielectric loss at low frequencies and it becomes low when the frequency reaches to a high value.

References

1. X.B. Chen, S.S.Mao, Chemical Reviews 7 (2007) 2891-2959.
2. Q. Pang, L. Leng, L. Zhao, L. Zhou, C. Liang, Y. Lan, Materials chemistry and physics 125 (2011) 612-616.
3. H. G.Yu, J.G.Yu. B. Cheng, J. Lin, Journal of Hazardous materials 147 (2007) 581-587.
4. N.R. Mathews, M.A.C. Jacome, E.R. Morales, J.A.T Antoniom, Physica status solidi, 6(2009) 219-223.
5. Grac, Zakeeruddin SM. Materials Today 2013; 16: (1-18).
6. N. Prabavathy, S. Shalini, R. Balasundaraprabhu et.al J.Mater Sci: Mater Electron springer science, Business media New York 2017.
7. H. Hug, M. Bader, P. Mair, T. Glat zel, Biophotovoltaics; Appl. Energy 115, 216-225 (2014).
8. G. K. Kaleji, J. Sol-Gel sci. Technol, 67 (2013) 312-320.
9. S. Benkara, S. Zerkout, H. Ghamri Materials Science in semi conductor processing 16(2013) 1271-1279.
10. O. wang, H. Fiang, S. Zang, Li. Q. Wang, J. Alloys comp. 586 (2014) 411 -419.
11. Jimin Du, Guoyan Zhao et al., Materials letters 93 (2013) 419-422.
12. N. Baram, D. Starosvetsky, M. Eptstein etal Electrochem. Comm., Vol(9), 7, (2007), 1684 -1688.
13. R.W. Mathews, J. Phys. Chem., Vol (91), 12, (1987), 3328-3333.
14. D. Mitoraj, A. Jancyk, M. Strus, H. Kischetal Photochem Photobiol Sci., Vol.(6), 6, (2007) 642-648.
15. H. Kisch, G. Burgeth and W. Macy K, Visible Light Photocatalysis by a Titania Transition metal complex, Vol (56), (2004), 241-259.
16. Kim D., Hahn S., Oh S., Kim E. : Materials Letters 57, 355 (2002).
17. Popov, O.A., Physics of Thin film Series, (Eds M.H. Francombe and J. Vossen), Vol.18 PP.122, Academic press, 1991.
18. E. R. Ollotu, M.E. Samiji, R.T. Kivaisi International journal of Nano science and Technology Vol.2, No.1 January 2014, PP 1-10, ISSN: 2328-5443.
19. P.C.Lansaker, P.Petersson, G.A. Niklasson & C.G. Grangvist. Solar energy materials and solar cells 117 (2013) 462-470.
20. M.O. Abou -Helal and W.T. Seeber, Appl. Surf. Sci., Vol(195), 1-4 (2002), 53-62.
21. N.C. Raut, T. Mathews, S.T. Sundari, T.N. Sairam S. Dash and A.K. Tyagi, J. Nanosci. Nanotechnol., Vol(9), 9,(2009), 5298-5302
22. L. Andronic, S. Manolache, and A. Duta, j. Optoelectron. Adv. Mater. Vol.(9), 5, (2007) 1403-1406.
23. D. Huang, S. Liao, S.Quan, L.Liu, Z.He, J.Wan and W. Zhou, J. Mater. Sci., Vol(42), 19, (2007), 8193-8202.
24. F.P. Huang and J.J. Sun, Proceedings of 3M-Nano International Conference, IEEE, Shaanxi, (2012), 97-101.
25. M. Effend and Bilslodin, J. Basci Appl. Sci., Vol (12), 2, (2012), 107-110.
26. R.C. Suciu, M.c.Rosu, T.D.Silips and A.R.Biris, Rev. Roum. Chim., Vol.(56), 6, (2011), 607-612.
27. N. Negishi, K. Takeuchi and T. Ibusuki, J. Sol-Gel Sci. Technol., Vol(13), 1-3, (1998) 691-694.
28. S.M. Attia, j.Wang, G.wu, J. Shen, and J. Ma., J. Mater Sci. Technol, Vol(18), 1, (2002). 31-33.
29. A.A. Daniyan, L.E. Umoru, B. Olunlade, J. Miner, Mater. Charac. Eng.1, 138(2013).
30. Liqun, M. Dinglin, L., HongxinD and Zhang,z. 2005. Materials Research Bullein. 40, 201-208.
31. Brinker. J. and Hurd, C.J., 1994, Fundamentals of Sol-Gel Dip-Coating, J. Phys. III France, 4, 1231.
32. Scherer, G.W., 1997, Sintering of Sol-Gel films, Journal of Sol-Gel Science and Technology, 8(1-3), 353-363.
33. Z. Ambrus, N. Balazs, T. Alapi, G. Wittmann, P.Sipos, A.Dombi, K. Mogyorosi, Applied Catalysis B: Environmental, 81 (2007) 27-373.
34. Z.Li, B. hou, Y. XU, D.Wu, Y.sun, Journal of Materials Science, 40(2005) 3939-3943.
35. K.S. Hwang, Y.S.Jeon, K.O. Jeon, B.H.Kim, Optica Applicata, 35 ,(2005) 1-9.
36. C.L.Luu, Q.T. Nguyen, S.T. Ho, Advances in Natural Science: Nano Science and Nano Technology, 31 (2010) 1-5.
37. W.G.Lee, Seong Ili Woo, Iong C. Kim, S.H.Choi and Key Hwan O, Thin Solid films – 237 (1994) 105-111.
38. Zhongchun Wang, Ulf, Helmersson, Per-olov Kall ,Thin solid films, 405(2002)50-54.

39. Suchitra sen, S.Bourgeois, D.Chaumont, Thin solid films, 474 (2005) 245-249.
40. C.J.Ridge, P.J.Harrop, D.S.Champbell, Thin solid films,2 (1968) 185.
41. B.Karunakaran, R.T.Rajendra Kumar, C.Viswanathan, D.Mangalaraj, Sa. K. Narayandass and G.Mohan Rao, Cryst. Res. Technol, 38 (2003) 773-778.
42. P.Argall and A.Ajonscher, Thin solid films, 2 (1968) 185.
43. T.Sawada and H.Hasegava, Thin solid films, 56 (1979) 183.

